SUPPORTING MATERIAL

Cells actively stiffen fibrin networks by generating contractile stress

Karin A. Jansen, Rommel G. Bacabac, Izabela K. Piechocka, Gijsje H. Koenderink
Biological Soft Matter Group, FOM Institute AMOLF,
1098 XG Amsterdam, Netherlands

SUPPORTING INFORMATION

Materials and Methods

(−)-Blebbistatin (Sigma-Aldrich) was dissolved in methanol to a final concentration of 5 mM and stored at -20^{o}C. The drug was tested in a final concentration range of 2 to 100 μM. Controls in which we added methanol without blebbistatin in cell culture medium showed no effect on cell morphology at these concentrations. In contrast, there was a clear reduction of cell spreading with increasing blebbistatin concentration (data not shown).

To test the involvement of integrins in cell spreading and traction force generation, we added the integrin-binding peptide GRGDS (AnaSpec Inc., Seraing, Belgium) to a 3 mg/ml fibrin matrix with fibroblasts, once the cells were well-spread. This peptide should compete with integrin binding sites on fibrin (1-3). GRGDS was dissolved in 5% acetic acid at a concentration of 2 mM and stored at -20^{o}C. GRGDS was freshly diluted with CO_2-independent medium to a concentration of 20 μM and added to cell-populated gels after completion of cell spreading by exchanging this medium with the medium on top of the glass disc. The final GRGDS concentration was 10 μM, sufficient for maximal inhibition of integrin binding (1-3).

qPCR protocol

Cells were allowed to spread for 6 hours within gels of 1 mg/ml fibrin (denoted as "3D") at a cell density of 500#/μl. Medium was removed and replaced by 0.05% trypsin/EDTA (Invitrogen). The gels were incubated for ~10 min at 37^{o}C to dissolve the gels. The solutions were then spun down and the pellets were quick-frozen and stored at -80^{o}C. Cells cultured in tissue culture flasks (denoted as "2D") were trypsinized and collected by centrifugation. Cell pellets were quick-frozen and stored at -80ºC. Quantitative real time PCR (qPCR) analysis was performed as described elsewhere(4). Briefly, RNA was isolated from cells grown in 2D or 3D culture using TRIsure (Bioline) and precipitated in 2-propanol for 1 hour room temperature. 500 ng of RNA was DNaseI treated and used as a template to generate cDNA following the manufacturer's instructions (Quantitect-Qiagen, Venlo, the Netherlands) with a mixture of oligo dT and random primers at 42°C during 30 min. The resulting cDNA (10 μl) was diluted 1:20 and served as a template in real-time quantitative PCR assays (SYBR Green PCR Master Mix (ABI)). Quantification and normalization procedures are described in detail elsewhere (5). Briefly, the expression of the genes *rnapolii*, *hprt*, *gapdh* and *ef1a* were used to normalize the detected integrin expression. Primers were designed for the PCR product to be intron spanning using NCBI's Primer Blast (6). qPCR was performed for integrin β3 with primers FW: CCCCACCACAGGCAATCAAA, and RV: AGCGTCAGCACGTGTTTGTA, and for integrin αV with primers FW: CAAGGGAACCCTTCCTCGGA, and RV: GGAGAAACAGTGCTCGTCGG.

Rheology

For rheology measurements of (cell seeded) fibrin gels, a steel cone and plate (40-mm diameter, 1°) was used. After 10 minutes, the fibrin gel was overlaid with 8 mL of αMEM supplemented with 2% FBS, 20 mM HEPES, and 0.1% antibiotics, as sketched in Fig. 1*A*. Since the medium is only touching the edges of the geometry, there will be a gradient of nutrients and oxygen from the sample edge to the center. To assess whether this gradient influences cell viability, we imaged cells within fibrin networks in a custom-made glass sample chamber that mimics the cone-plate geometry of the rheometer. Based on cell morphology, we counted the number of spread, round and dead cells (Fig. S1). We found that up to about 10 mm inwards (corresponding to half the radius of the geometry), the cells are spread. At 8-9 mm inwards, the fraction of round cells starts to go up. At about 12 mm inwards, cells start to die, mostly likely due to an oxygen and metabolite gradient. Thus, clearly, cells do not behave the same in the center as near the edge. It should be noted, however, that in a cone-plate geometry, the outer edges contribute much more strongly to the measured mechanics than the center of the sample. Also in the region where the cells do spread, more than 80% of the sample volume is located. We also note that even if the CP40-1 geometry is not ideal for cell survival, it does create a three-dimensional scaffold for the cells and is therefore a reasonable compromise between cell survival and three-dimensionality, with the effect of dead cells on fibrin gel mechanics being minimal. We also checked that the presence of medium around the rheometer plates did not influence the viscoelastic behavior.

PIV analysis

Particle Image Velocimetry **(**PIV) analysis was performed based on fluorescence confocal microscopy time-lapse movies of 2 and 3 mg/ml fibrin gels recorded during cell spreading. We used an existing PIV routine in Matlab (PIVlab_GUI.m, downloaded from *http://www.mathworks.nl*). Briefly, 1064x1064 pixels images were highpass filtered using a filter size of 15 to 30 pixels before analysis. PIVlab uses a method called 'multiple pass' to increase accuracy. The search window area at step one was 64 pixels with 32 pixel overlap, at step two 32 with 18 pixels overlap and at step three 20 with 10 pixels overlap.The last step is chosen to be slightly bigger than the observed meshsize. For finding of the peak of the correlation matrix, a Gaussian 2x3 point sub-pixel estimator was used. The final accuracy was estimated to be 1 to 2 μm, corresponding to a few pixels (7).

Alignment analysis

To analyze the response of fibrin fiber orientations to the presence of cells, we analyzed confocal images of cell-free and cell-populated fibrin networks using the ImageJ plugin OrientationJ, developed by Daniel Sage at the Biomedical Image Group (BIG), EPFL, Switzerland and freely available at bigwww.epfl.ch *(last visited 26 August 2013)*. Specifically, we analyzed maximum intensity projections of z-scans taken over a depth of 40 μm (1 μm step size). Briefly, OrientationJ evaluates the local orientation and coherency of every image pixel and computes a distribution of angles. A Gaussian window of 2 or 3 pixels and a Gaussian gradient was used to determine the local derivative (8). Using these orientation images, we calculated the nematic order parameter. Given a collection of orientation measurements, θ, in the range (-90º, 90º], the nematic order parameter is computed from the second-order tensor order-parameter S_2(9):

$$S_2 = \begin{bmatrix} \langle \cos 2\theta \rangle & \langle \sin 2\theta \rangle \\ \langle \sin 2\theta \rangle & -\langle \cos 2\theta \rangle \end{bmatrix}$$

.

Angle brackets <·> denote averages over all orientation measurements. The tensor S_2 is symmetric and traceless. Solving the eigenvalue problem for S_2 yields two eigenvalues,

$$\lambda_{1,2} = \pm\sqrt{\langle \cos 2\theta \rangle^2 + \langle \sin 2\theta \rangle^2} = \pm S$$

which yield the (two-dimensional) scalar order-parameter S familiar for liquid crystals. This order parameter quantifies the width of the distribution of orientation measurements. It is zero for a uniform distribution of orientations, and approaches one for a sharply-peaked distribution. We find that in practice S is between 0.1 and 0.2 for isotropic networks.

SUPPORTING REFERENCES

1. Tuan, T., and F. Grinnell. 1989. Fibronectin and fibrinolysis are not required for fibrin gel contraction by human skin fibroblasts. J. Cell Physiol. 140:577-583.
2. Gailit, J., C. Clarke, D. Newman, M. Tonnesen, M. Mosesson, and R. Clark. 1997. Human fibroblasts bind directly to fibrinogen at RGD sites through integrin αVβ3. Exp. Cell Res. 232:118-126.
3. Campbell, R., K. Overmyer, C. Selzman, B. Sheridan, and A. Wolberg. 2009. Contributions of extravascular and intravascular cells to fibrin network formation, structure, and stability. Blood 114:4886-4896.
4. Kamphuis, W., C. Mamber, M. Moeton, L. Kooijman, J. Sluijs, A. Jansen, M. Verveer, L. deGroot, V. Smith, S. Rangarajan, J. Rodríguez, M. Orre, and E. Hol. 2012. GFAP isoforms in adult mouse brain with a focus on neurogenic astrocytes and reactive astrogliosis in mouse models of Alzheimer disease. PLoS One 7:e42823.
5. Dijk, F., E. Kraal-Muller, and W. Kamphuis. 2004. Ischemia-induced changes of AMPA-type glutamate receptor subunit expression pattern in the rat retina: a real-time quantitative PCR study. Invest. Ophthalmol. Vis. Sci. 45:330-341.
6. Ye, J., G. Coulouris, I. Zaretskaya, I. Cutcutache, S. Rozen, and T. Madden. 2012. Primer-BLAST: a tool to design target-specific primers for polymerase chain reaction. BMC Bioinformatics 13:134.
7. Noguera, J., A. Lecuona, and P. Rodríguez. 2005. Limits on the resolution of correlation PIV iterative methods. Fundamentals. Experiments in Fluids 39:9.
8. Rezakhaniha, R., A. Agianniotis, J. Schrauwen, A. Griffa, D. Sage, C. Bouten, F. vandeVosse, M. Unser, and N. Stergiopulos. 2011. Experimental investigation of collagen waviness and orientation in the arterial adventitia using confocal laser scanning microscopy. Biomech. Model Mechanobiol. 11:461-473.
9. Hess, S., and W. Köhler. 1980. Formeln zur Tensor-Rechnung. Palm & Enke.

SUPPORTING FIGURES

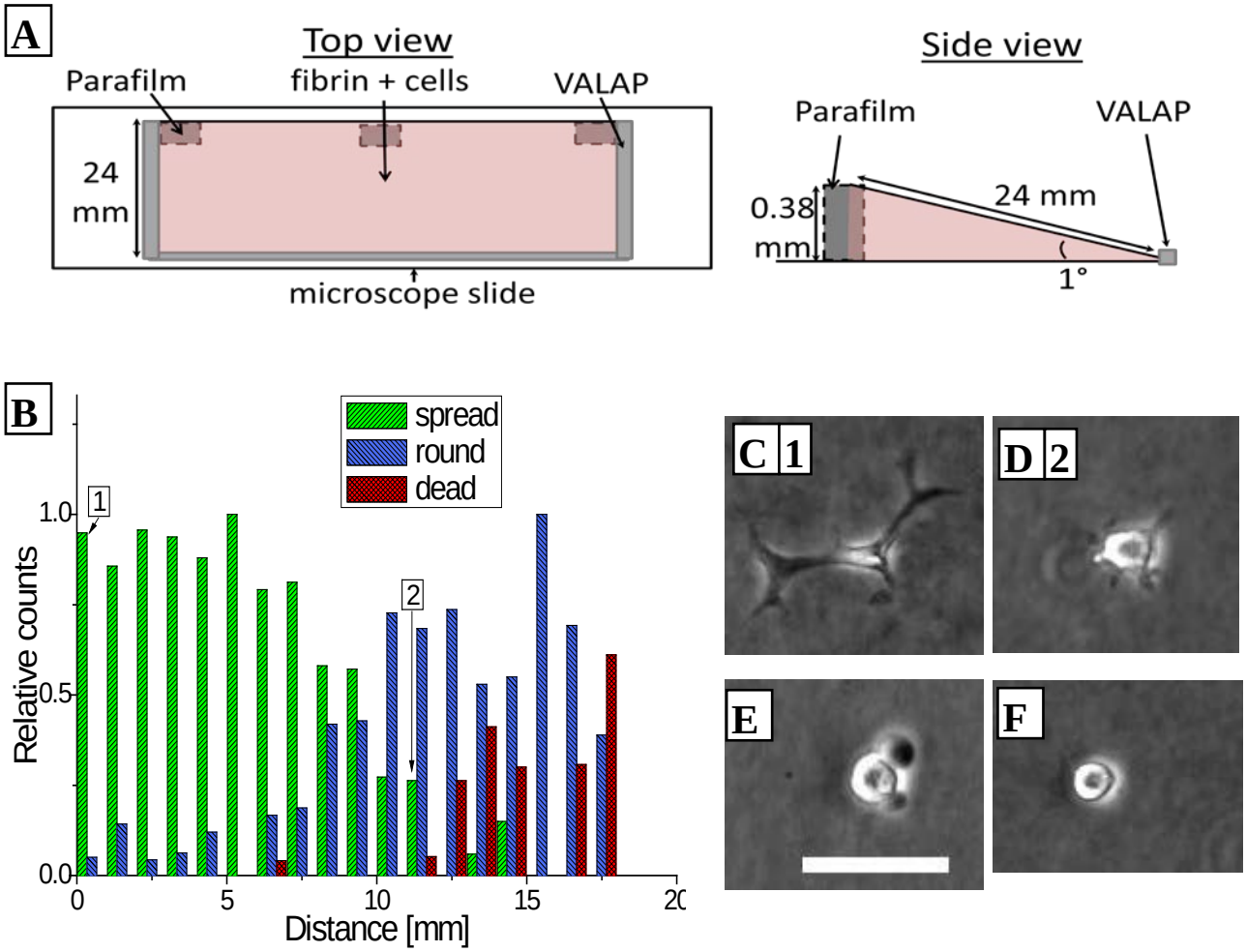

FIGURE S1 (*color online)* Morphologies of cells in a 2 mg/ml fibrin gels after 7 hours in a sample geometry that mimics the rheometer cone-plate geometry. A) Schematic showing how the CP40-1 geometry is mimicked using glass coverslips (not drawn to scale). After filling the geometry with a solution of activated fibrinogen and cells, the sides were sealed with VALAP and the geometry was placed in a petridish with medium after 10 minutes polymerization. Cells were observed in the middle of the glass slide. B) Relative counts of spread (*green)*, round *(blue)* and dead cells *(red)* as a function of distance from the edge, as determined from cell morphology. C-F) Examples of cell morphologies observed with a 10x air objective using phase contract. C) and D) represent 'spread' morphologies seen at spot 1 and 2 in B). E) Example of a dead cell. F) Example of a round cell. The scale bar is 50 μm for all images.

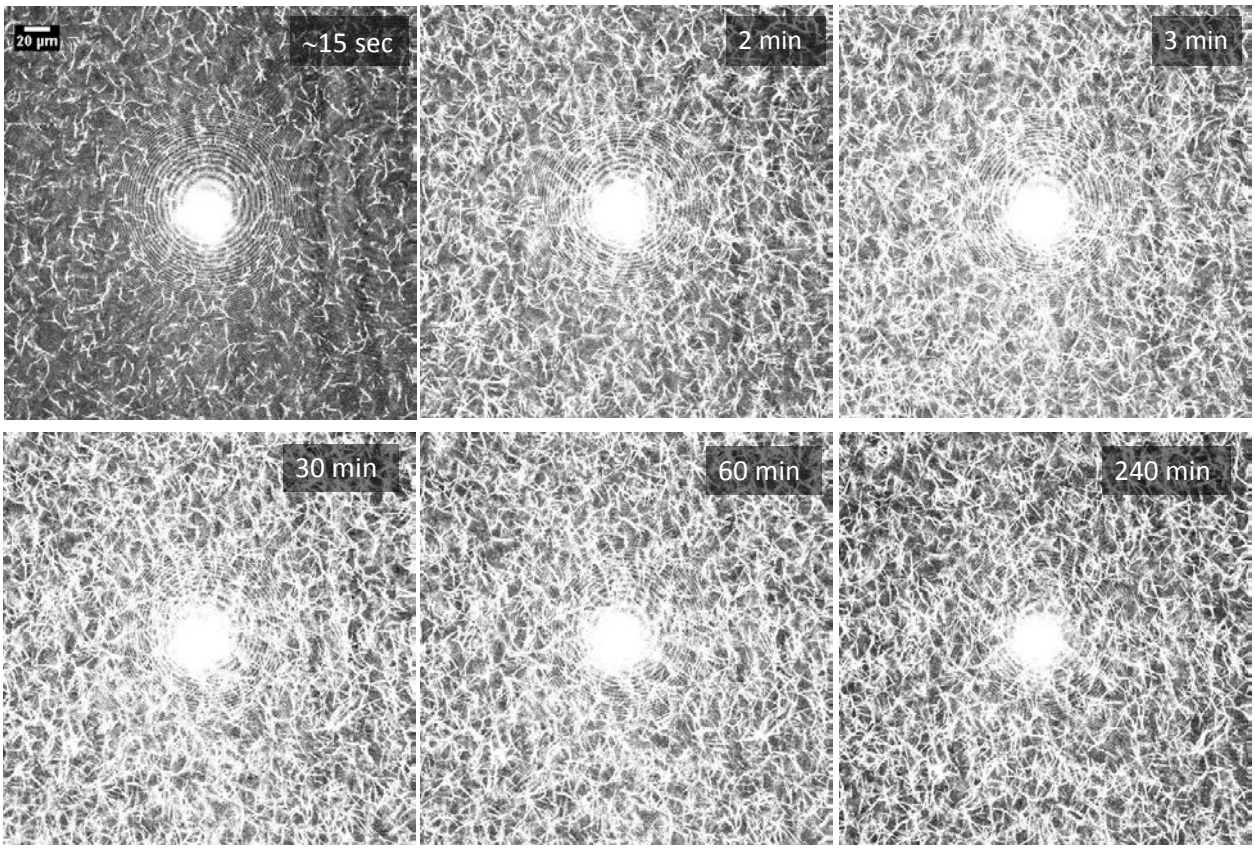

FIGURE S2. Time lapse images showing polymerization of a cell-free fibrin gel recorded by label-free confocal reflection microscopy (1 mg/ml). The scale bar denotes 20 μm. Images were taken using a 40x oil objective and 457 nm laser light. Time elapsed since the addition of thrombin is indicated in each panel. The bright spot in the center is an artifact of the imaging technique. Images recorded after the 15 second time point are over-saturated because the laser and detector settings were optimized to capture the earliest time point.

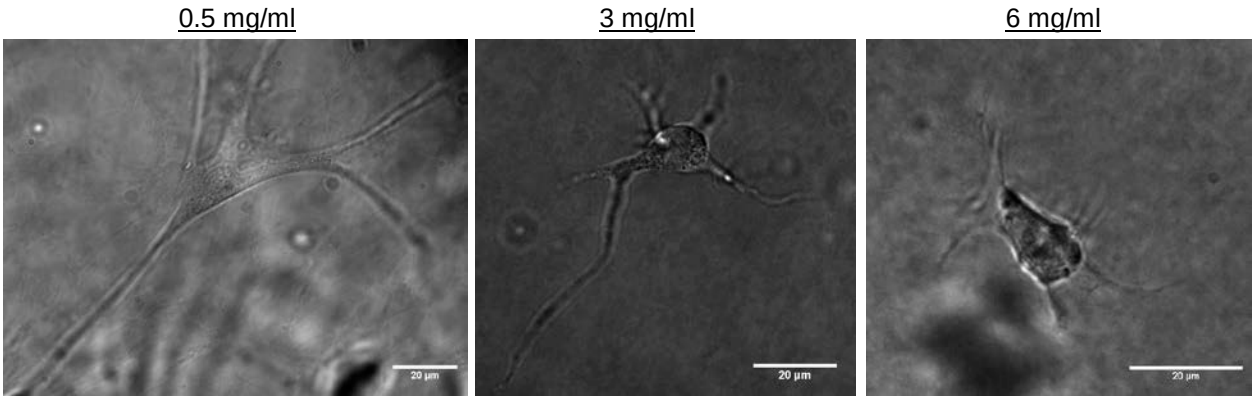

FIGURE S3. Cells in fibrin gels of different concentrations (see labels) imaged using a 40x oil immersion objective. Images were taken after overnight incubation. The scale bars are 20 μm.

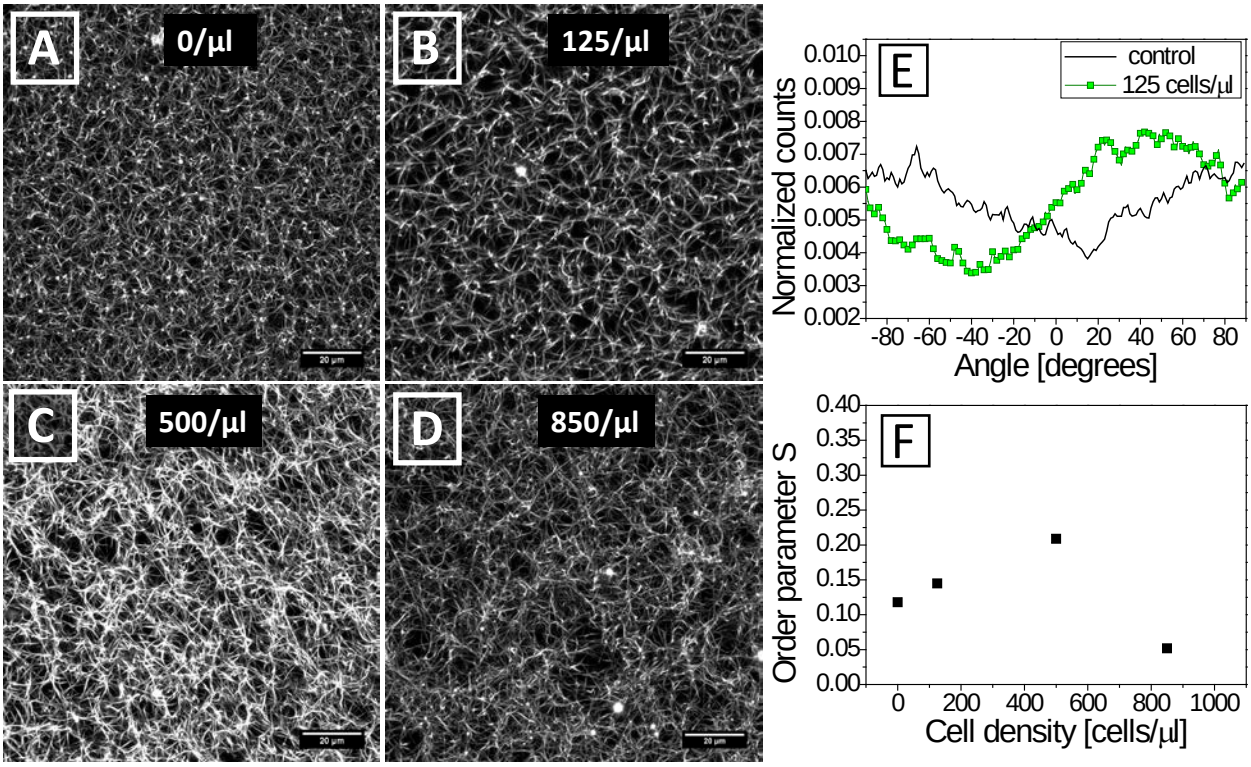

FIGURE S4. The effect of increasing cell density (see labels) on fibrin network structure. (A)-(D) All images are maximum intensity projections of confocal fluorescence microscopy stacks of 40 images spanning 40 µm in height. The cell density was varied from 0 to 850 cells/µl (see labels). Scale bars are 20 µm. (E) Pixel orientation histogram for images (A) (control, *black line*) and (B) (*green line squares*). Images were analyzed using OrientationJ. (F) Nematic order parameter of images (A-D). S can range between 0 for an isotropic system and 1 for a perfectly aligned system, but in practice we find values of 0.1-0.2 for isotropic networks. Only the networks with 500 cells/µl is slightly anisotropic (S = 0.21).

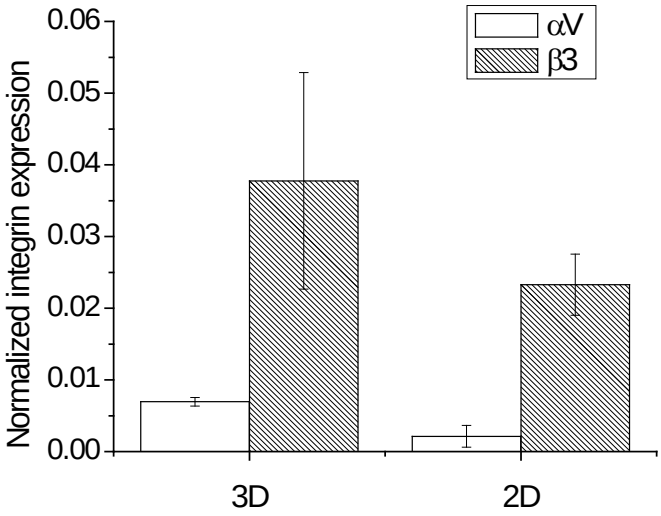

FIGURE S5. Normalized expression of integrins αV and β3 (see legend) for CCL224 fibroblasts cultured inside a fibrin gel (3D) or in flasks (2D). The measurements were performed using qPCR.

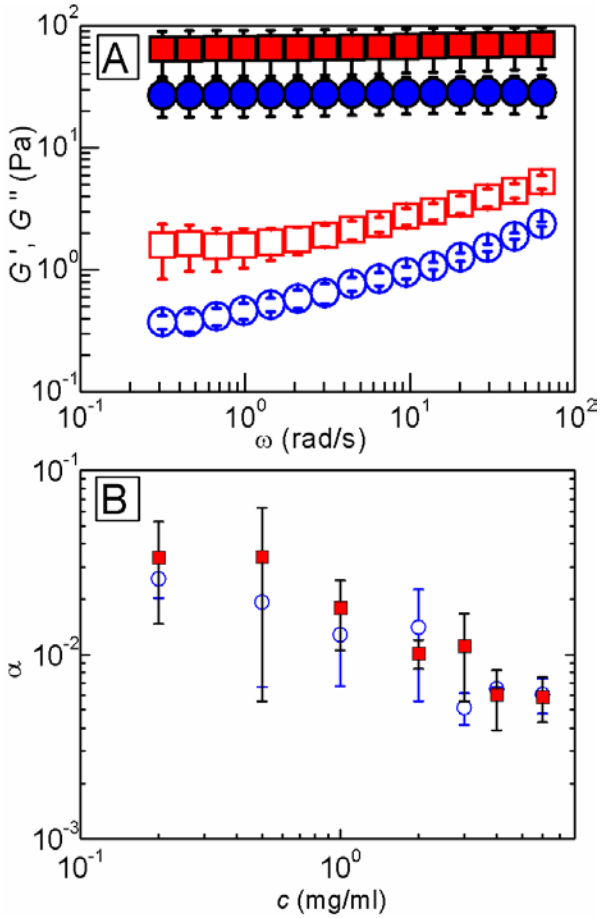

FIGURE S6. (*color online*) Frequency dependence of the linear rheology of fibrin gels with cells (red squares) and without cells (blue circles). (A) Linear elastic modulus (solid symbols) and viscous modulus (open symbols) of a fibrin network (1 mg/ml) with and without cells (500 /μl). (B) Power law exponent, α, of the frequency dependent elastic modulus for fibrin networks with and without cells (500/μl) as a function of fibrin concentration.

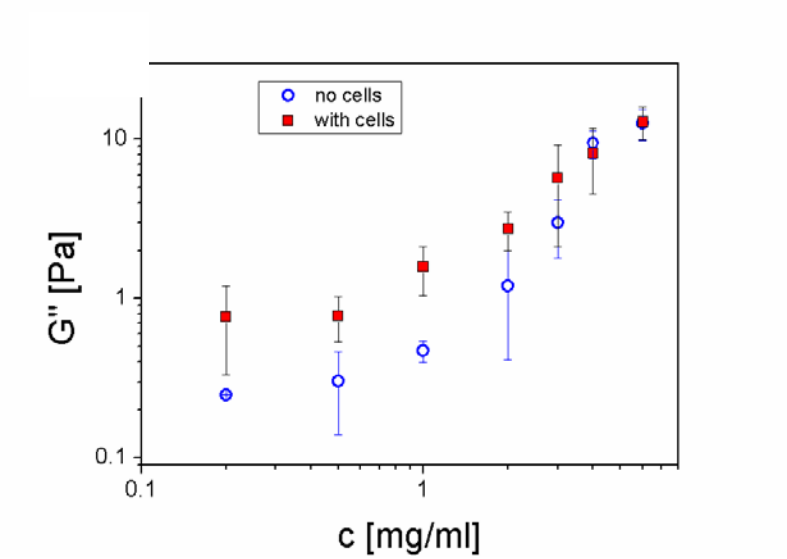

FIGURE S7. (*color online*) The viscous (loss) modulus *G''* of cell-seeded (500/µl) fibrin gels (red solid squares) and unseeded fibrin gels (blue open circles) as a function of fibrin concentration.

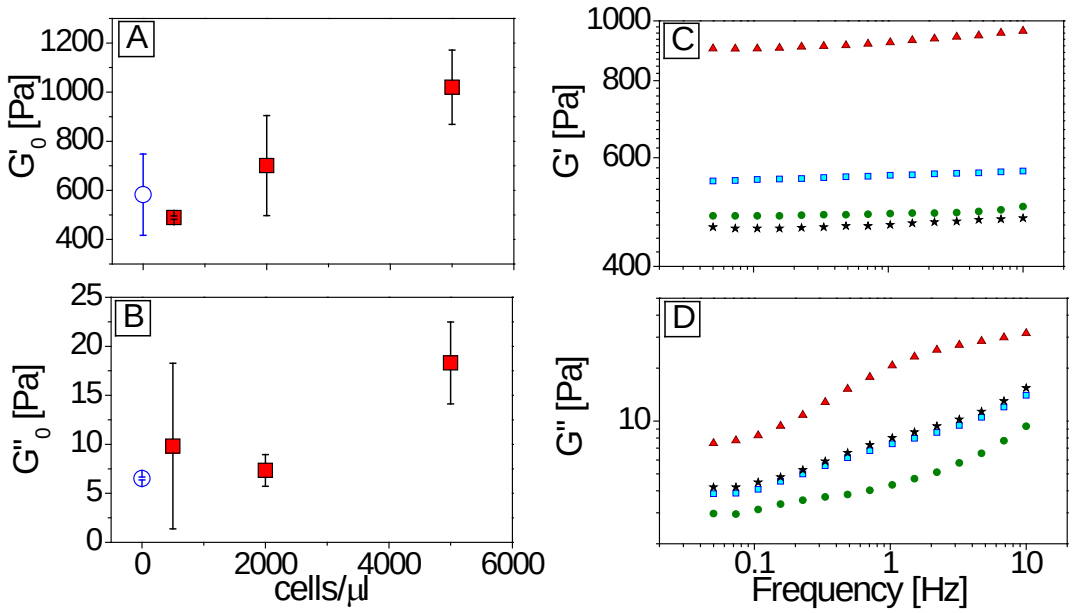

FIGURE S8 (*color online*) (A-B) The elastic (storage) plateau modulus, G_0', and viscous (loss) modulus G_0'' of cell-seeded fibrin gels (red solid squares) and unseeded fibrin gels (blue open circles) as a function of cell density for a 4 mg/ml fibrin gel. (C-D) The frequency dependence of cell-seeded fibrin gels (green filled circles 500 cells/µl, blue squares 2000 cells/µl, red triangles 5000 cells/µl) and unseeded fibrin gels (black stars) as a function of cell density for a 4 mg/ml fibrin gel. The frequency dependence is unaffected, except at 5000 cells/µl. Perhaps the volume fraction of cells is large enough here to influence the overall rheology.

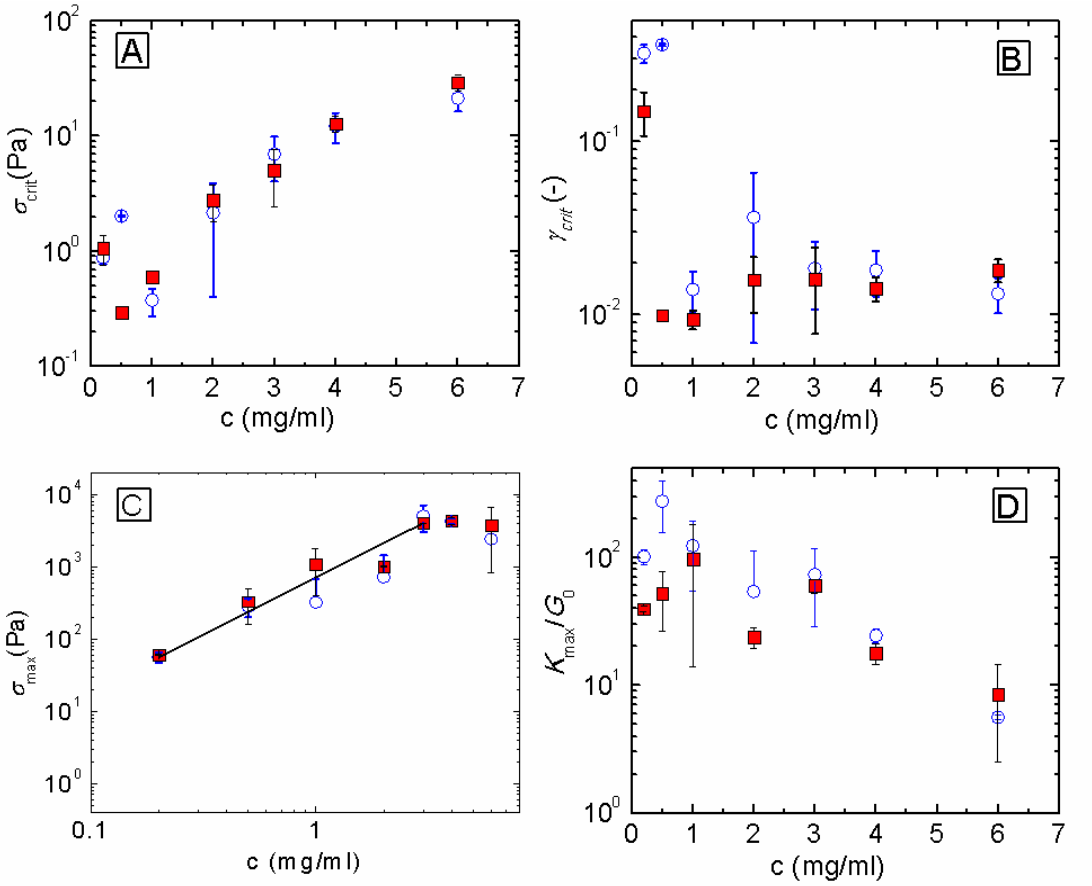

FIGURE S9 (*color online*) Critical stress (A) and critical strain (B), maximum shear stress (C) and the maximum extend of strain-stiffening before breakage (K_{max}/G_0, (D)), plotted against fibrin concentration. Open circles correspond to unseeded gels, while closed squares correspond to gels with 500 cells/µl. The line in (C) shows a power-law fit with an exponent of 1.6 ±0.14.

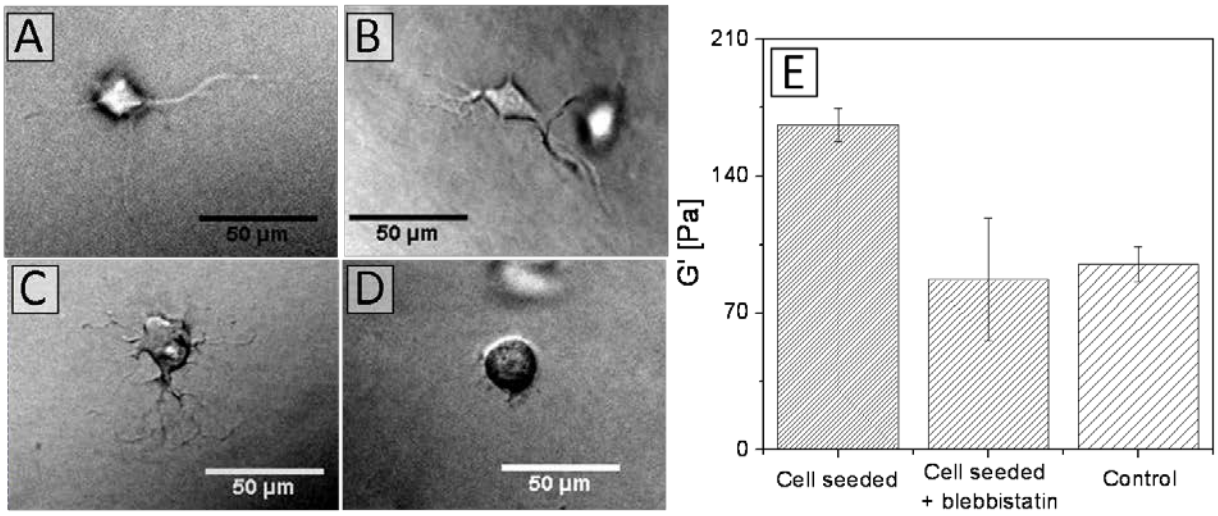

FIGURE S10. Effect of blebbistatin on cell spreading and fibrin gel mechanics. (A)-(D) Typical cell morphologies of cells in 2 mg/ml fibrin gels after 7 hours of spreading in the absence (A) or in the presence of blebbistatin (2, 40 and 100 μM in panels (B), (C), (D), respectively). Images were taken in bright field using a 10x air objective. Scale bar is 50 μm for all images. (E) Fibrin gel stiffness with and without cells in the presence or absence of blebbistatin. Blebbistatin was added in the medium from the start to a final concentration of 100 μM. In case of the control sample (no cells), we added methanol without blebbistatin. For the cell seeded case there was no methanol added to the medium. However, tests in 2D culture showed no effect on cell spreading at this methanol concentration. Data points are averages of 4 separate measurements for the control and of two separate measurements for the other two cases.

MOVIE CAPTIONS

Movie S1 Time-lapse movie of a fibroblast spreading inside a network of 0.5 mg/ml fibrin. The movie starts 10 min after starting fibrin polymerization and the total duration is 9 hours. The frame rate is 1 frame/min. Images were taken using a bright field microscope with a 10×/0.3 N.A. air objective.

Movie S2 Time-lapse movie of a fibroblast spreading inside a network of 6 mg/ml fibrin. The movie starts 10 min after starting fibrin polymerization and the total duration is 9 hours. The frame rate is 1 frame/min. Images were taken using a bright field microscope with a 10×/0.3 N.A. air objective.

Movie S3 3D-Reconstruction of a confocal fluorescence microscopy z-stack consisting of 93 slices spaced 300 nm apart of a 1 mg/ml fibrin gel with an embedded fibroblast, 4 hours after polymerization. Images were taken using a confocal microscope with a 100× oil immersion objective.

Movie S4 Time-lapse movie of a fibroblast spreading inside a 1 mg/ml fibrin network seeded with fiducial markers (1 μm diameter polystyrene beads) that reveal the influence of cell contraction on the surrounding fibrin network. The total duration is 4 hours, and the frame rate is 1 frame/min. As the cell spreads, it pulls the beads inward, starting about 1 hour after fibrin polymerization.

Movie S5 Time-lapse movie showing that addition of the RGD peptide GRGDS causes an abrupt release of tension in the fibrin matrix surrounding a fully spread fibroblast; the cell rounds up and the fiducial markers (5 μm diameter polystyrene beads) near the cell are displaced. The fibrin concentration is 3 mg/ml. The total duration is 9 hours, and the frame rate is 1 frame/min. Images were taken using a bright field microscope with a 10×/0.3 NA air objective and extra magnification of 1.5x.

Movie S6 Time-lapse movie of fibroblasts spreading inside a 2 mg/ml fibrin gel. Cells are imaged by DIC (*top left*), while the fibrin network is imaged by confocal fluorescence microscopy (*top right*). The deformation of the fibrin network during cell spreading is evident from the PIV analysis shown in the bottom left corner. The total duration is 7.5 hours, the frame rate is 1 frame/10 min. Images were taken with an inverted Nikon confocal microscope with a 40x oil immersion objective and a 488 nm laser. The scale bar denotes 100 μm for all movies.

Movie S7 Time-lapse movie of fibroblasts spreading inside a 3 mg/ml fibrin gel. Cells are imaged by DIC (*top left*), while the fibrin network is imaged by confocal fluorescence microscopy (*top right*). There is no evident network deformation at timescales up to 7.5 hour, as shown with PIV analysis (*bottom left corner*). The total duration is about 9 hours, the frame rate is 1 frame/10 min. Images were taken with an inverted Nikon confocal microscope with a 40x oil immersion objective and a 488 nm laser. The scale bar denotes 100 μm for all movies. The color scale for the PIV analysis indicates the velocity in pixels/10min.